Inorg. Chem. **2002**, *41*, 6426–6431

Synthesis and Structural Characterization of Di- and Tetranuclear Zinc Complexes with Phenolate and Carboxylate Bridges. Correlations between ^{13}C NMR Chemical Shifts and Carboxylate Binding Modes

Bao-Hui Ye,*,† Xiao-Yuan Li,‡ Ian D. Williams,‡ and Xiao-Ming Chen†

School of Chemistry & Chemical Engineering, Sun Yat-Sen University, Guangzhou, 510275, P. R. China. Department of Chemistry, The Hong Kong University of Science and Technology, Clear Water Bay, Kowloon, Hong Kong, P. R. China

Received June 19, 2002

Two di- and a tetranuclear zinc–carboxylate complexes with different coordination modes, $[Zn_2L(\mu_{1,3}\text{-}OAc)_2](ClO_4)$ (**1**), $[Zn_2L(\mu_{1,3}\text{-}Pro)_2](ClO_4)$ (**2**), and $[Zn_2L(\mu_{1,1}\text{-}HCO_2)(\mu_{1,3}\text{-}HCO_2)]_2(ClO_4)_2$ (**3**) (where L = 2,6-bis(*N*-2-(2′-pyridylethyl)-formimidoyl)-4-methylphenol, OAc = acetate, and Pro = propionate) have been synthesized. Their compositions and structures have been identified by elemental analyses, IR, NMR, and X-ray single-crystal diffraction. The cations in both **1** and **2** reveal that the two zinc ions are assembled by a phenolate and a pair of syn–syn $\mu_{1,3}$-carboxylate bridges with metal–metal distances of 3.281 and 3.331 Å, respectively, and each polyhedron around the zinc ion is a slightly distorted trigonal bipyramid. Compound **3** is a tetranuclear complex consisting of two identical dinuclear subunits that connect to each other by the two formate groups. In each subunit, the pair of metal ions separated at 3.130(1) Å is assembled by a phenolate oxygen from L, and a monodentate and a syn–syn bidentate formate bridges. The formate group displays a novel tridentate mode, namely, monodentate and syn–anti bidentate bridges. On the other hand, the solid-state ^{13}C NMR technique was employed to distinguish the different binding modes of acetate group in five-coordinate zinc complexes. The chemical shifts are as follows: chelating mode (ca. 184 ppm) > bidentate bridge (ca. 180 ppm) > monodentate bridge (ca. 176 ppm).

Introduction

The zinc ion is of essential importance in several biological processes. Apart from enzymes with one zinc binding site, such as carbonic anhydrase and carboxypeptidase A, enzymes containing two or three zinc ions at the active sites are currently of particular interest.[1] The most important and distinguishing features in these zinc enzymes are that the two ions are connected to each other through one solvent molecule (OH^- or H_2O) as well as the carboxylate function from amino acid side chains with the Zn···Zn distances from 3.0 to 3.5 Å.[2−6] The catalytic role of zinc ion is ascribed to the orientation and activation of substrates; the bridging groups keep the two metal ions at a suitable distance and give a fundamental contribution to substrate activation.

In zinc enzymes, the carboxylate groups exhibit monodentate terminal (**I**), bidentate chelating (**II**), bidentate bridging (**IIIa**), and monodentate bridging (**IIIb**) coordination modes[7] (Chart 1). Numerous examples from experiment and calculation have proved that "carboxylate shift" is a low-energy path in the altering of binding mode in catalytic cycles of metalloenzymes.[7,8] In the course of synthesis and char-

* Author to whom correspondence should be addressed. Telephone: (86)-20-84113986. Fax: (86)-20-84112245. E-mail: cesybh@zsu.edu.cn.
† Sun Yat-Sen University.
‡ The Hong Kong University of Science and Technology.

(1) (a) Lipscomb, W. N.; Sträter, N. *Chem. Rev.* **1996**, *96*, 2375. (b) Wilcox, D. E. *Chem. Rev.* **1996**, *96*, 2435. (c) Sträter, N.; Lipscomb, W. N.; Klabunde, T.; Krebs, B. *Angew. Chem., Int. Ed. Engl.* **1996**, *35*, 2024. (d) Steinhagen, H.; Helmchem, G. *Angew. Chem., Int. Ed. Engl.* **1996**, *35*, 2339.
(2) Sträter, N.; Lipscomb, W. N. *Biochemistry* **1995**, *34*, 14792.
(3) Chevrier, B.; Schalk, C.; D'Orchymont, H.; Rondeau, J.; Moras, D.; Tarnus, C. *Structure* **1994**, *2*, 283.
(4) Vanhooke, J. L.; Benning, M. M.; Raushel, F. M.; Holden, H. V. *Biochemistry* **1996**, *35*, 6020.
(5) Hough, E.; Hansen, L. K.; Birknes, B.; Jynge, K.; Hansen, S.; Hordvik, A.; Little, C.; Dodson, E.; Derewenda, Z. *Nature* **1989**, *338*, 360.
(6) Volbeda, A.; Lahm, A.; Sakiyama, F.; Suck, D. *EMBO J.* **1991**, *10*, 1607.
(7) Rardin, R. L.; Tolman, W. B.; Lippard, S. J. *New. J. Chem.* **1991**, *15*, 417.
(8) (a) Herold, S.; Lippard, S. J. *Inorg. Chem.* **1997**, *36*, 50. (b) LeCloux, D. D.; Barrios, A. M.; Mizoguchi, T. J.; Lippard, S. J. *J. Am. Chem. Soc.* **1998**, *120*, 9001. (c) Voegtli, W. C.; Khidekel, N.; Baldwin, J.; Ley, B. A.; Bollinger, J. M.; Rosenzweig, A. C. *J. Am. Chem. Soc.* **2000**, *122*, 3255.

10.1021/ic025806+ CCC: $22.00
Published on Web 10/31/2002

Chart 1. Carboxylate Binding Modes in Zinc Enzymes

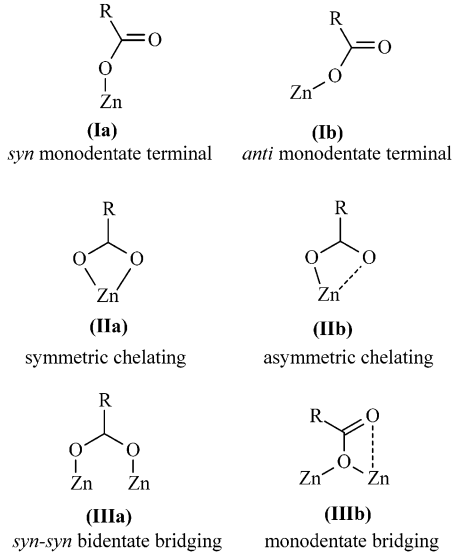

acterization model complexes with different binding modes of carboxylate,[9] the question of how to use the simple spectral techniques to distinguish the binding modes of carboxylate ligand always puzzled us. Deacon and Phillips have carefully examined the IR spectra of many carboxylate complexes with known X-ray crystal structures and drawn useful conclusions for the correlations between $\nu(CO_2)$ frequencies and carboxylate geometries.[10] Unfortunately, the conclusions do not apply to identification of the chelating mode from the bidentate bridging mode and sometimes give the reverse results. On the other hand, ^{1}H and ^{19}F NMR spectra have already been employed to identify the **IIIa** and **IIIb** binding modes in the paramagnetic cobalt and iron complexes.[11] Recently, variable-temperature ^{1}H NMR technique have been successfully applied to observe the "carboxylate shift" directly in solution, but the ^{13}C NMR spectrum failed to resolve the binding modes.[12] Nevertheless, a trinuclear complex $[Zn_3(py)_2(OAc)_6]$ containing two different carboxylate binding modes showed only one type resonance peak in solution.[13] In fact, the ^{13}C NMR spectrum may serve as a potential technique for diagnosing the binding modes since it markedly depends on the bonding electrons' bond orders and on electron densities and can be employed to observe the chemical shift of the carbonyl group directly. Indeed, the carboxylate group with **I** and **II** modes as axial ligand in porphyrine have been clearly identified by ^{13}C NMR spectra.[14] We have also tried to apply the solid-state ^{13}C NMR technique to diagnose the binding modes of carboxylate in dimagnesium complex, in which we found that the **Ia** and **IIIa** modes displayed different chemical shifts.[9c] As a continuation of this observation, we describe herewith the syntheses and structural characterization of two di- and a tetranuclear zinc−carboxylate complexes with different coordination modes, $[Zn_2L(\mu_{1,3}\text{-}OAc)_2](ClO_4)$ (**1**), $[Zn_2L(\mu_{1,3}\text{-}Pro)_2](ClO_4)$ (**2**), and $[Zn_2L(\mu_{1,1}\text{-}HCO_2)(\mu_{1,3}\text{-}HCO_2)]_2(ClO_4)_2$ (**3**) (where L = 2,6-bis(*N*-2-(2′-pyridylethyl)formimidoyl)-4-methylphenol, OAc = acetate, and Pro = propionate), to observe the correlations between the metal−metal separations and the bridged ligands. Compound **3** provides a good structural model at the active site of leucine aminopeptidase from bovine lens,[2] and the formate group presents a novel coordination fashion in metal carboxylate chemistry. Furthermore, the ^{13}C cross-polarization/magic angle spinning (CP/MAS) spectrum was employed to diagnose the binding modes of carboxylate.

Experimental Section

Materials and Methods. All starting materials were purchased from commercial sources and were used without further purification. $Zn(Pro)_2\cdot 2H_2O$ was prepared by the reaction of ZnO and propionic acid in 1:2 ratio in aqueous at room temperature. The synthesis and crystal structure of $[Zn_2(bipy)_2(\mu_{1,1}\text{-}OAc)(\mu_{1,3}\text{-}OAc)_2](ClO_4)$ (bipy = 2,2′-bipyridine) has been reported previously.[9d] Elemental analyses (C, H, and N) were performed on a Perkin-Elmer 240Q elemental analyzer. FT-IR spectra were recorded on a Bruker IFS-66 or Perkin-Elmer 16 spectrometer using KBr pellet method (400−4000 cm^{-1}). ^{1}H and ^{13}C NMR spectra were recorded on a Bruker ARX-300 NMR spectrometer in CD_3CN solution at room temperature; the CD_3CN signal was used to lock the field, and all chemical shifts are given relative to tetramethylsilane (TMS); ^{1}H NMR spectra were measured at 300.132 MHz, and ^{13}C NMR spectra were obtained 74.475 MHz using CD_3CN as an internal standard with wide band proton decoupling. The cross-polarization and magic spinning (CPMAS) ^{13}C NMR spectrum was detected on a Joel-400 MHz spectrometer in solid state at room temperature; ^{13}C NMR spectra were acquired at 400.40 MHz with a spectral width of 40 kHz, 8K real data points, and a recycle time of 7s, using adamentane (ADM) as an external standard, and the chemical shifts are referenced to TMS.

*Caution***!** Although no problem was encountered in the preparation of the perchlorate salt, care should be taken when handing such a potentially explosive compound.

Synthesis of $[Zn_2L(\mu_{1,3}\text{-}OAc)_2](ClO_4)$ (1). 2-(Aminoethyl)-pyridine (0.244 g, 2 mmol) was added to the solution of 2,6-diformyl-4-methylphenol (0.164 g, 1 mmol) in methanol (15 mL). After stirring at 40 °C for 0.5 h, $Zn(OAc)_2\cdot 2H_2O$ (0.219 g, 2 mmol) was added. The resulting solution was stirred at 40 °C for an additional 3 h, then $NaClO_4$ (0.244 g, 2 mmol) was added, and the above solution was further stirred for another 1 h. The reaction mixture was filtered, and the methanol solvent was removed by rotatory evaporation under reduce pressure. A small amount of CH_3CN was added to dissolve the residue and ethyl acetate was dropped to afford **1**. The pure product was obtained by recrystallization from

(9) (a) Ye, B.-H.; Mak, T.; Williams, I. D.; Li, X.-Y. *Chem. Commun*. **1997**, 1813. (b) Schultz, B. E.; Ye, B.-H.; Li, X.-Y.; Chan, S. I. *Inorg. Chem*. **1997**, *36*, 2617. (c) Ye, B.-H.; Mak, T.; Williams, I. D.; Li, X.-Y. *J. Chem. Soc., Dalton Trans.* **1998**, 1935. (d) Chen, X.-M.; Tong, Y.-X.; Mak, T. C. W. *Inorg. Chem*. **1994**, *33*, 4586.

(10) Deacon, G. B.; Phillips, R. J. *Coord. Chem. Rev*. **1980**, *33*, 227.

(11) (a) Hagen, K. S.; Lachicotte, R. J. *J. Am. Chem. Soc*. **1992**, *114*, 8741. (b) Lachicotte, R. J.; Kitagorodskiy, A.; Hagen, K. S. *J. Am. Chem. Soc*. **1993**, *115*, 8883. (c) Hagen, K. S.; Lachicotte, R. J.; Kitagorodskiy, A. *J. Am. Chem. Soc*. **1993**, *115*, 12617. (d) Nair, V. S.; Hagen, K. S. *Inorg. Chem*. **1994**, *33*, 185. (e) Hagen, K. S.; Lachicotte, R. J.; Kitagorodskiy, A.; Elbouadili, A. *Angew. Chem., Int. Ed. Engl*. **1993**, *32*, 1321. (f) Lachicotte, R. J.; Hagen, K. S. *Inorg. Chim. Acta* **1997**, *263*, 407.

(12) Demšar, A.; Košmrlj, J.; Petriček, S. *J. Am. Chem. Soc*. **2002**, *124*, 3951.

(13) Singh, B.; Long, J. R.; deBiani, F. F.; Gatteschi, D.; Stavropoulos, P. *J. Am. Chem. Soc*. **1997**, *119*, 7030.

(14) Lin, S.-J.; Hong, T.-N.; Tung, J.-Y.; Chen, J.-H. *Inorg. Chem*. **1997**, *36*, 3886.

CH_3CN and ethyl acetate solution. Yield 0.596 g, 82.8%. FT-IR data (KBr, cm^{-1}): 1648 (vs), 1633 (vs), 1596 (vs), 1570 (s), 1551 (s), 1490 (m), 1445 (vs), 1411 (s), 1339 (m), 1237 (m), 1092 (vs, br), 765 (s), 666 (m), 622 (s). ^1H NMR data (CD_3CN, ppm): 8.66 (2H, d, $J = 5.6$ Hz, py-H_6), 8.46 (2H, s, ph-CH═N), 8.01 (2H, t, py-H_4), 7.54−7.50 (4H, m, py-H_3 or py-H_5), 7.46 (2H, s, ph-H_3 or ph-H_5), 4.07 (4H, t, N−CH_2–C), 3.36 (4H, t, C−CH_2–py), 2.35 (3H, s, ph-CH_3) and 1.93 (6H, s, OAc−CH_3). ^{13}C NMR data (CD_3CN, ppm): 180.20, 171.64, 165.72, 160.52, 149.13, 142.98, 139.64, 125.00, 124.70, 122.90, 120.31, 60.13, 35.42, 22.69 and 18.49. Anal. Calcd for $C_{27}H_{29}ClN_4O_9Zn_2$: C, 45.04; H, 4.03; N, 7.78. Found: C, 45.15; H, 4.12; N, 7.82%. A single-crystal suitable for X-ray diffraction was obtained by diffusing the CH_3CN solution of **1** into ethyl acetate.

$[Zn_2L(\mu_{1,3}$-Pro$)_2](ClO_4)$ (2) was synthesized by the procedure similar to that of **1** using $Zn(Pro)_2 \cdot 2H_2O$ in place of $Zn(OAc)_2 \cdot 2H_2O$. Yield 0.59 g, 79%. FT-IR data (KBr, cm^{-1}): 1646 (vs), 1630 (vs), 1588 (vs), 1568 (vs), 15481 (s), 1484 (m), 1442 (vs), 1414 (s), 1348 (m), 1238 (m), 1092 (vs, br), 1036 (m), 816 (m), 776 (m), 624 (vs). ^1H NMR data (CD_3CN, ppm): 8.63 (2H, d, $J =$ 5.4 Hz, py-H_6), 8.46 (2H, s, ph-CH═N), 8.00 (2H, t, py-H_4), 7.53−7.48 (4H, m, py-H_3 or py-H_5), 7.46 (2H, s, ph-H_3 or ph-H_5), 4.08 (4H, t, N−CH_2–C), 3.36 (4H, t, C−CH_2–py), 2.34 (3H, s, ph-CH_3), 2.23 (4H, q, Pro-CH_2) and 0.91 (6H, t, Pro-CH_3). ^{13}C NMR data (CD_3CN, ppm): 183.15, 171.65, 165.73, 160.53, 149.06, 142.99, 139.54, 124.97, 124.62, 122.78, 120.30, 60.15, 35.43, 29.56, 18.49 and 9.27. Anal. Calcd for $C_{29}H_{33}ClN_4O_9Zn_2$: C, 46.54; H, 4.41; N, 7.49. Found: C, 46.61; H, 4.54; N, 7.62%. A single-crystal suitable for X-ray diffraction was obtained by diffusing the CH_3CN solution of **2** into ethyl acetate.

$[Zn_2L(\mu_{1,1}$-$HCO_2)(\mu_{1,3}$-$HCO_2)]_2(ClO_4)_2$ (3). 2-(Aminoethyl)-pyridine (0.122 g, 1 mmol) was added to the solution of 2,6-diformyl-4-methylphenol (0.082 g, 0.5 mmol) in methanol (10 mL). After stirring at 40 °C for 0.5 h, HCO_2Na (0.136 g, 2 mmol) was added. Then, $Zn(ClO_4)_2 \cdot 6H_2O$ (0.372 g, 1 mmol) was added to the above solution, and the resulting solution was stirred at 40 °C for additional 3 h. The reaction mixture was filtered, and the methanol solvent was removed by rotatory evaporation under reduced pressure. A small amount of CH_3CN was added to dissolve the residue, and ethyl acetate was dropped to afford **3**. The pure product was obtained by recrystallizing from CH_3CN and ethyl acetate solution. Yield 0.26 g, 75.3%. FT-IR data (KBr, cm^{-1}): 1648 (vs), 1634 (vs), 1606 (vs), 1582 (vs), 1570 (s), 1554 (s), 1488 (m), 1446 (s), 1414 (s), 1362 (m), 1320 (m), 1240 (m), 1090 (vs, br), 774 (m), 766 (m), 624 (s), 622 (s). ^1H NMR data (CD_3CN, ppm): 8.66 (2H, d, $J = 5.2$ Hz, py-H_6), 8.47 (2H, s, ph-CH═N), 8.28 (2H, s, HCO_2), 8.02 (2H, t, py-H_4), 7.55−7.50 (4H, m, py-H_3 and py-H_5), 7.48 (2H, s, ph-H_3 and ph-H_5), 4.09 (4H, t, N−CH_2–C), 3.38 (4H, t, C−CH_2–py) and 2.35 (3H, s, ph-CH_3). ^{13}C NMR data (CD_3CN, ppm): 171.78, 169.87, 165.70, 160.48, 149.08, 142.23, 139.79, 125.31, 124.89, 122.98, 120.30, 60.11, 35.48 and 18.47. Anal. Calcd for $C_{50}H_{50}Cl_2N_8O_{18}Zn_4$: C, 43.39; H, 3.62; N, 8.10. Found: C, 43.56; H, 3.73; N, 8.23%. A single-crystal suitable for X-ray diffraction was obtained by diffusing the CH_3CN solution of **3** into ethyl acetate.

X-ray Crystallography and Structure Solution. Crystal data as well as data collection and refinement for complexes are summarized in Table 1. Single crystals with approximate dimensions 0.3 × 0.3 × 0.3 (**1**), 0.20 × 0.22 × 0.34 (**2**), and 0.5 × 0.5 × 0.6 mm (**3**) were mounted, respectively, on a glass fiber, and placed on a Enraf-Nonius CAD-4 (**2**) or Siemens P4 (**1** and **3**) diffractometer equipped a low-temperature device. Intensity data were obtained by using Mo Kα radiation (0.710 73 Å) monochromatized from a graphite crystal. For each complex, determination of the crystal class, orientation matrix, and cell dimensions were performed according to the established procedures. Three standard reflections were monitored after every 100−150 data measurements, showing only small random variations. The crystal structures were solved by the direct methods with the aid of successive difference Fourier maps and refined with full-matrix least-squares using either the SHELXTL IRIS[15] (**1** and **3**) or teXsan[16] (**2**) program package. Atomic scattering factors were taken from the *International Table for X-ray Crystallography*. The four oxygen atoms of the perchlorate group in **1** and the atoms O(9), C(7), C(12), C(16), and C(17) in **3** exhibit 2-fold orientational disorder. All the non-hydrogen atoms were refined anisotropically. All hydrogen atoms were generated at ideal positions (C−H = 0.96 Å), and fixed with isotropic thermal parameters.

Table 1. Crystallographic and Experimental Data for **1**-**3**

	1	**2**	**3**
empirical formula	$C_{27}H_{29}ClN_4O_9Zn_2$	$C_{29}H_{33}ClN_4O_9Zn_2$	$C_{50}H_{50}Cl_2N_8O_{18}Zn_4$
fw	719.7	749.8	1382.6
cryst syst	Monoclinic	Triclinic	Triclinic
space group	$P2_1/n$	$P\bar{1}$ (No. 2)	$P\bar{1}$ (No. 2)
a (Å)	8.517(2)	10.744(1)	11.214(1)
b (Å)	17.902(2)	13.038(1)	11.888(1)
c (Å)	19.347(2)	13.901(2)	11.925(1)
α (deg)		114.67(1)	74.88(1)
β (deg)	101.15(23)	106.38(2)	64.28(1)
γ (deg)		100.43(1)	82.22(1)
V (Å^3)	2894.2(8)	1594.8(5)	1382.2(4)
Z	4	2	2
ρ_{calcd} (g cm^{-3})	1.652	1.557	1.657
T (K)	228	298	298
λ(Mo Kα) (Å)	0.710 73	0.710 73	0.710 73
μ(Mo Kα) (cm^{-1})	18.10	16.46	18.91
R1 ($I > 2\sigma(I)$)[a]	0.0396	0.0340	5.86
wR2[a]	0.0449	0.0350	7.73

[a] $R1 = \sum||F_o| - |F_c||/\sum|F_o|$; $wR2 = [\sum w(|F_o| - |F_c|)^2/\sum w|F_o|^2]^{1/2}$.

Results and Discussion

Synthesis. The Zn···Zn separations at the active site of enzymes fall in the range of 3.0−3.5 Å,[1−6] and these distances have been believed to be primarily governed by the bridging ligands, such as the solvent molecule (H_2O or OH^-) and the carboxylate ligand. Such a problem has been nicely resolved through designing and synthesis of efficient zinc model complexes with different ligands.[17−20] Uhlebrock and Krebs have reported the first example of dizinc complex with a phenoxo-bridge as a model at the active site of

(15) Sheldrick, G. M. *SHELXTL-IRIS*; Siemens Analytical X-ray Instruments Inc.: 1993.

(16) *Crystal Structure Analysis Package;* Molecular Structure Corp.: 1985 and 1992.

(17) (a) Kimura, E.; Koike, T. *Adv. Inorg. Chem*. **1994**, *39*, 1. (b) Fenton, D. E.; Okawa, H. *Chem. Ber*. **1997**, *130*, 433.

(18) Chaudhuri, P.; Stockheim, C.; Wieghardt, K.; Deck, W.; Gregorzik, R.; Vahrenkamp, H.; Nuber, B.; Weiss, J. *Inorg. Chem*. **1992**, *331*, 1451.

(19) (a) Tanase, T.; Yun, J. W.; Lippard, S. J. *Inorg. Chem*. **1995**, *34*, 4220. (b) Tanase, T.; Yun, J. W.; Lippard, S. J. *Inorg. Chem*. **1996**, *35*, 3585. (c) Tanase, T.; Yun, J. W.; Lippard, S. J. *Inorg. Chem*. **1996**, *35*, 7590. (d) Koike, T.; Inoue, M.; Kimura, E.; Shiro, A. *J. Am. Chem. Soc*. **1996**, *118*, 3091. (e) Chapman, W. H. Jr.; Breslow. R. *J. Am. Chem. Soc*. **1995**, *117*, 5462. (f) Bazzicalupi, C.; Bencini, A.; Bianchi, A.; Fusi, V.; Giorgi, C.; Paoletti, P.; Valtancoli, B.; Zanchi, D. *Inorg. Chem*. **1997**, *36*, 2784. (g) Uhlenbrock, S.; Wenger, R.; Krebs, B. *J. Chem. Soc., Dalton Trans*. **1996**, 3731.

(20) (a) Uhlenbrock, S.; Krebs, B. *Angew. Chem., Int. Ed. Engl*. **1992**, *31*, 1647. (b) Reim, J.; Krebs, B. *J. Chem. Soc., Dalton Trans*. **1997**, 3793.

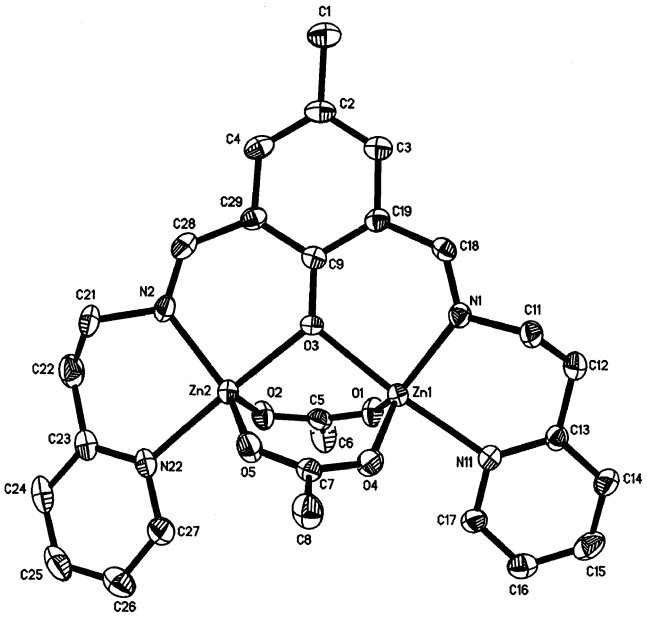

Figure 1. Molecular structure and atomic numbering scheme for cation $[Zn_2L(\mu_{1,3}\text{-}OAc)_2]^+$ in **1**. Ellopsoids are drawn at the 40% probability level.

phospholipase C.[20] Here another phenoxo-bridged ligand L has been synthesized by condensation of 2,6-diformyl-4-methylphenol and 2-(aminoethyl)-pyridine in methanol solution at 40 °C, which could be used as a binuclear ligand. Two homo-dinuclear and a tetranuclear zinc complexes containing a phenoxo and two carboxylate bridges have been prepared to observe the correlations between the metal−metal separations and the bridged ligands. On the other hand, the zinc complexes with different binding modes of carboxylate, such as **IIa**, **IIIa**, and **IIIb**, have also been prepared and employed to observe the correlations between ^{13}C NMR chemical shifts and the binding modes of carboxylate.

Crystal Structures. (a) $[Zn_2L(\mu_{1,3}\text{-}OAc)_2](ClO_4)$ (1) and $[Zn_2L(\mu_{1,3}\text{-}Pro)_2](ClO_4)$ (2). The crystal structures of **1** and **2** consist of $[Zn_2L(\mu_{1,3}\text{-}OAc)_2]^+$ or $[Zn_2L(\mu_{1,3}\text{-}Pro)_2]^+$ cations and perchlorate anions. In the cation, the dizinc ions are assembled by a phenolate oxygen and a pair of syn−syn carboxylate bridges as shown in Figure 1. The selected bond distances and angles of the both complexes are collected in Table 2. Each of the two zinc ions is further coordinated by two nitrogen atoms form the L ligand, forming two ZnN_2O_3 polyhedra joined at their shared vertex by the oxygen atom of the phenoxo-bridging in a face-to-face fashion. The Zn···Zn separations in **1** (3.281 Å) and **2** (3.331 Å) are comparable to those observed in triple bridged model complexes $[Zn_2(bipy)_2(\mu_{1,1}\text{-}OAc)(\mu_{1,3}\text{-}OAc)_2]^+$ (3.275 Å)[9d] and $[Zn_2(\mu\text{-}OH)(\mu_{1,3}\text{-}OAc)_2(Me_3tacn)_2]^+$ (3.311 Å),[18] and in the zinc enzymes such as phosphotriesterase from *P. diminuta* (3.3 Å),[4] phospholipase C from *Bacillus cereus* (3.3 Å),[5] and nuclease P1 from *P. citrinum* (3.2 Å),[6] but slightly shorter than those observed in the double bridged complex $[Zn_2(bbap)(\mu_{1,3}\text{-}OAc)(H_2O)]^+$ (3.443 Å).[20]

In both complexes, each of the zinc ions is a pentacoordinated species and the polyhedron around the Zn ion can be best described as a slightly distorted trigonal−bipyraminal geometry.[21] At Zn(1), O(3) of the phenolate oxygen and N(11) from the pyridyl ring occupy at the axial positions with the angle of O(3)−Zn(1)−N(11) at 173.3(1) and 179.6(1)° for **1** and **2**, respectively, while N(1), O(1), and O(4) atoms are in the trigonal plane. In the Zn(2), the two axial sites are occupied by the O(3) and N(22) from other pyridyl ring with the angle of O(3)−Zn(2)−N(22) at 178.0(1) and 177.3(2)° for **1** and **2**, respectively, and the N(2), O(2), and O(5) atoms lie in the equatorial plane. As expected for an ideal trigonal bipyramid, all Zn ions lie within the trigonal planes (average deviation from the four-atom plane is ca. 0.04 Å). In both complexes, the bond distances at axial position are significant longer than those in the equatorial plane.

Table 2. Selected Bond Distances (Å) and Angles (deg) for **1** and **2**

	1	**2**
Zn(1)−N(1)	2.019(4)	2.030(4)
Zn(1)−N(11)	2.191(4)	2.195(5)
Zn(1)−O(1)	1.979(3)	1.980(4)
Zn(1)−O(3)	2.128(3)	2.147(3)
Zn(1)−O(4)	1.965(3)	1.984(4)
Zn(2)−N(2)	2.024(4)	2.016(6)
Zn(2)−N(22)	2.163(4)	2.200(4)
Zn(2)−O(2)	2.006(3)	1.975(4)
Zn(2)−O(3)	2.091(3)	2.129(3)
Zn(2)−O(5)	1.996(3)	1.988(4)
N(1)−Zn(1)−N(11)	89.9(1)	91.1(2)
N(1)−Zn(1)−O(1)	126.1(1)	113.9(2)
N(11)−Zn(1)−O(1)	85.8(1)	89.2(2)
N(1)−Zn(1)−O(3)	87.0(1)	88.5(1)
N(11)−Zn(1)−O(3)	173.3(1)	179.6(1)
O(1)−Zn(1)−O(3)	91.3(1)	91.0(1)
N(1)−Zn(1)−O(4)	112.9(1)	123.4(2)
N(11)−Zn(1)−O(4)	90.4(1)	88.3(1)
O(1)−Zn(1)−O(4)	120.8(1)	122.6(2)
O(3)−Zn(1)−O(4)	96.2(1)	91.8(1)
N(2)−Zn(2)−N(22)	92.9(2)	90.2(2)
N(2)−Zn(2)−O(2)	113.0(1)	120.9(2)
N(22)−Zn(2)−O(2)	86.7(1)	90.4(2)
N(2)−Zn(2)−O(3)	89.1(1)	88.4(1)
N(22)−Zn(2)−O(3)	178.0(1)	177.3(2)
O(2)−Zn(2)−O(3)	92.7(1)	92.3(1)
N(2)−Zn(2)−O(5)	122.3(1)	122.0(2)
N(22)−Zn(2)−O(5)	88.8(1)	86.1(2)
O(2)−Zn(2)−O(5)	124.6(1)	116.9(2)
O(3)−Zn(2)−O(5)	90.0(1)	92.7(1)

(b) $[Zn_2L(\mu_{1,1}\text{-}HCO_2)(\mu_{1,3}\text{-}HCO_2)]_2(ClO_4)_2$ (3). A perspective view of the cation in **3** is depicted in Figure 2a. The geometry of the tetranuclear core emphasizing the arrangement of the zinc ions and the binding modes of the carboxylates is shown in Figure 2b. Selected interatomic distances and angles are given in Table 3.

Compound **3** can be described as a tetranuclear complex consisting of two identical dinuclear $[Zn_2L(\mu_{1,1}\text{-}HCO_2)(\mu_{1,3}\text{-}HCO_2)]^+$ subunits which connect to each other via the coordination of the dangling oxygen form the formate to the zinc of other subunit. The two zinc ions within a subunit are bridged by a phenolate oxygen O(3), and a monodentate O(8) and an additional syn−syn bidentate of formates with a 3.130(1) Å distance. Although a number of dinuclear zinc complexes have been prepared, the species that contains a

(21) Addison, A. W.; Rao, T. N.; Reedijk, J.; Rijn, J. van; Vershoor, G. C. *J. Chem. Soc., Dalton Trans.* **1984**, 1349.

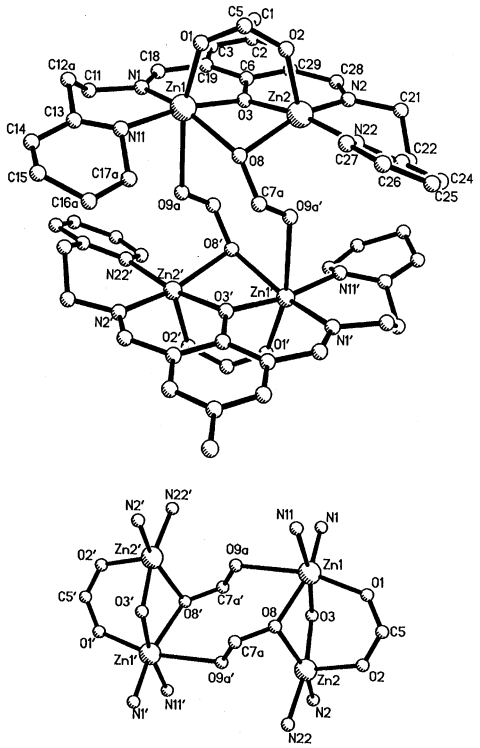

Figure 2. (a) Molecular structure and atomic numbering scheme for cation $[Zn_2L(\mu_{1,1}\text{-}HCO_2)(\mu_{1,3}\text{-}HCO_2)]_2^{2+}$ in **3**. (b) Inner coordination sphere for the zinc ions in **3** emphasizing the coordination modes of formate groups.

Table 3. Selected Bond Distances (Å) and Angles (deg) for **3**

Zn(1)−N(1)	2.014(4)	Zn(1)−N(11)	2.098(6)
Zn(1)−O(1)	2.034(6)	Zn(1)−O(3)	2.057(3)
Zn(1)−O(8)	2.211(5)	Zn(1)−O(9a)	2.469(9)
Zn(2)−N(2)	2.010(4)	Zn(2)−N(22)	2.099(5)
Zn(2)−O(2)	2.008(6)	Zn(2)−O(3)	2.048(3)
Zn(2)−O(8)	2.152(5)	Zn(1)···Zn(2)	3.130(1)
Zn(1)···Zn(1)	5.889	Zn(1)···Zn(2)	5.085
Zn(2)···Zn(2)	6.053		
N(1)−Zn(1)−N(11)	95.0(2)	N(1)−Zn(1)−O(1)	108.2(2)
N(11)−Zn(1)−O(1)	95.2(3)	N(1)−Zn(1)−O(3)	89.8(2)
N(11)−Zn(1)−O(3)	170.6(3)	O(1)−Zn(1)−O(3)	90.9(2)
N(1)−Zn(1)−O(8)	157.8(3)	N(11)−Zn(1)−O(8)	93.8(2)
O(1)−Zn(1)−O(8)	91.3(2)	O(3)−Zn(1)−O(8)	78.9(2)
N(1)−Zn(1)−O(9a)	86.8(2)	N(11)−Zn(1)−O(9a)	88.1(3)
O(1)−Zn(1)−O(9a)	164.2(2)	O(3)−Zn(1)−O(9a)	84.1(2)
O(8)−Zn(1)−O(9a)	73.1(2)	N(2)−Zn(2)−N(22)	95.0(2)
N(2)−Zn(2)−O(2)	109.0(2)	N(22)−Zn(2)−O(2)	93.5(2)
N(2)−Zn(2)−O(3)	89.7(1)	N(22)−Zn(2)−O(3)	170.2(2)
O(2)−Zn(2)−O(3)	93.1(2)	N(2)−Zn(2)−O(8)	157.4(2)
N(22)−Zn(2)−O(8)	92.1(2)	O(2)−Zn(2)−O(8)	91.9(2)
O(3)−Zn(2)−O(8)	80.5(2)		

μ-hydroxo (oxo, water, alkoxo, or phenoxo), a μ_{11}-carboxylate and a syn−syn $\mu_{1,3}$-carboxylate within a dinuclear unit is very rare. Therefore, this provides a good model at the active site of leucine aminopeptidase from bovine lens,[2] in which the two zinc ions are connected by a hydroxo (or water), a monodentate oxygen from Asp255, and a syn−syn bidentate oxygen from Glu334 with a comparable distance of 3.0 Å. This Zn···Zn separation is significantly shorter than those observed in other zinc enzymes (3.2−3.5 Å)[3−6] and the model complexes, such as **1** (3.281 Å), **2** (3.331 Å), $[Zn_2(bbap)(\mu_{1,3}\text{-carboxylate})(H_2O)]^{2+}$ (3.443 Å),[21] $[Zn_2(bipy)_2(\mu_{1,1}\text{-OAc})(\mu_{1,3}\text{-OAc})_2]^+$ (3.275 Å),[9d] $[Zn_2(bdmap)(\mu_{1,1}\text{-OAc})(\mu_{1,3}\text{-OAc})_2]_2$ (3.215 Å),[12] and $[Zn_2(\mu\text{-OH})(\mu_{1,3}\text{-OAc})_2(Me_3tacn)_2]^+$ (3.311 Å).[18] It is notable that the metal−metal distance is mainly governed by the nature, number, and geometry of the bridged ligands, especially by the monatomic bridge.

Chart 2. Carboxylate Binding Modes Intridentate Fashion

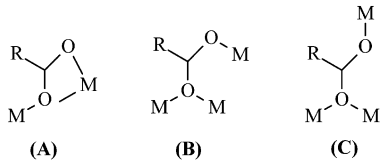

It is interesting that the two zinc ions display two different coordination geometries within a dinuclear subunit. The Zn(2) ion is a five-coordinate via three oxygen atoms from a phenolate and two formate groups, and further via two nitrogen atoms from the L ligand, forming a ZnN_2O_3 distorted square pyramid with the O(2) at axial position. While Zn(1) is a six-coordinate by an additional coordination of O(9) atom [Zn(1)−O(9a) = 2.469 (9) Å] from the another formate, resulting in a ZnN_2O_4 distorted octahedral environment. The distance of Zn(1)−O(8) [2.211(5) Å] is slightly longer than that of Zn(2)−O(8) [2.152(5) Å]. This can be attributed to the fact that the former is a six-coordinate while the latter is a five-coordinate.

The most interesting observation is that there are two binding modes for the formate groups in **3**, namely, syn−syn bidentate and tridentate bridges. The former is most common in dinuclear or polynuclear metal carboxylate chemistry.[22] On the contrary, tridentate bridge is rare in a metal−carboxylate complex.[7] As shown in Chart 2, there are three modes in tridentate bridges. The mode **A** is postulated to be an important intermediate in "carboxylate shift" chemistry,[7] and mode **B** (a monodentate and a syn−syn bidentate bridges) have also been found in metal carboxylate chemistry.[23] The present study provides a novel example with mode **C** geometry, in which the formate displays in a tridentate mode with a monodentate and a syn−anti bidentate bridges. The mode **C** geometry is very rare due to the fact that the anti electron lone pairs of the carboxylate group have a lower basicity than the syn one.[24]

Infrared and NMR Spectra. IR spectra of **1**−**3** all display the characteristic bands of carboxylate at 1582−1606 cm^{-1} for $\nu_{as}(CO_2)$ and ca. 1412 cm^{-1} for $\nu_s(CO_2)$. Furthermore, there are two bands at 1606 and 1582 cm^{-1} for $\nu_{as}(CO_2)$ in **3** corresponding to two binding modes of formate. The frequency differences (Δ) between $\nu_{as}(CO_2)$ and $\nu_s(CO_2)$ are 185 cm^{-1} for **1**, 174 cm^{-1} for **2**, and 192 and 168 cm^{-1} for **3**, respectively, which are slightly larger than that observed in ionic complex of carboxylate (Δ = 164 cm^{-1}).[10] However,

(22) Mehrotra, R. C.; Bohra, R. *Metal Carboxylate*; Academic Press: New York, 1983.
(23) Prout, C. K.; Carruthers, J. R.; Rossotti, F. J. *J. Chem. Soc. A* **1971**, 3350. Post, M. L.; Trotter, J. *J. Chem. Soc., Dalton Trans.* **1974**, 674. Mounts, R. D.; Ogura, T.; Fernando, Q. *Inorg. Chem.* **1974**, *13*, 802. Bertaut, E. F.; Duc, T. Q.; Burlet, P.; Thomas, M.; Moreau, J. M. *Acta Crystallogr.* **1974**, *B30*, 2234. Freeman, H. C.; Huq, F.; Stephens, G. N. *J. Chem. Soc. Chem. Commun.* **1976**, 90. Cotton, F. A.; Lewis, G. E.; Mott, G. N. *Inorg. Chem.* **1983**, *22*, 1825. Clegg, W.; Little, T. R.; Straughan, B. P. *Inorg. Chem.* **1988**, *27*, 1916.
(24) Wiberg, K. B.; Laidig, K. E. *J. Am. Chem. Soc.* **1987**, *109*, 5935.

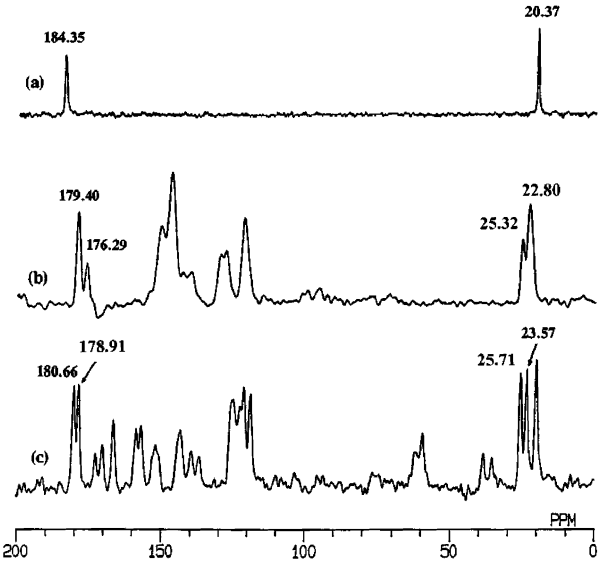

Figure 3. CPMAS ^{13}C NMR spectra of zinc complexes with different acetate binding modes (a) $Zn(OAc)_2(H_2O)$ in **II** mode with 363 scans, (b) $[Zn_2(bipy)_2(\mu_{1,1}\text{-OAc})(\mu_{1,3}\text{-OAc})_2](ClO_4)$ in **IIIa** and **IIIb** modes with 323 scans, and (c) **1** in **IIIa** mode with 674 scans in solid state at 25 °C.

the Δ values in some dizinc complexes with a syn−syn bidentate mode, such as $[Zn_2(bbap)(\mu_{1,3}\text{-carboxylate})(H_2O)]^{2+}$ (150 cm^{-1})[20] and $[Zn_2(bipy)_2(\mu_{1,1}\text{-OAc})(\mu_{1,3}\text{-OAc})_2]^+$ (155 cm^{-1}),[9d] show less than that of the ionic complex and are close to that of $Zn(OAc)_2(H_2O)$ (Δ = 145 cm^{-1}), in which the acetate groups display in a chelating mode.[25] Therefore, it is not feasible to distinguish the chelate mode (**IIa**) from the bidentate bridge mode (**IIIa**) only via IR data.

Notably, NMR technique can provide useful information to diagnose the binding modes of carboxylate group. NMR and IR spectroscopies provide complementary methods for investigating the binding modes of carboxylate. It is well-known that the ^{13}C chemical shift of carbonyl carbon not only depends on the coordination mode, but also on the coordination number of metal ion. To prevent the sample dissociating in solution and binding by solvent molecule and to ensure their structures correspondence to the results from X-ray single-crystal diffraction, ^{13}C NMR spectra of five-coordinate zinc complexes with different binding modes of acetate were recorded in the solid state (Figure 3). The ^{13}C NMR spectrum of $Zn(OAc)_2(H_2O)$ was shown in Figure 3a, in which acetate group display in a chelating mode (**IIa**),[25] and the downfield resonance peak at 184.35 ppm was assigned to the carbonyl group. Figure 3b shows the ^{13}C NMR spectrum of $[Zn_2(bipy)_2(\mu_{1,1}\text{-OAc})(\mu_{1,3}\text{-OAc})_2](ClO_4)$. There are two resonance peaks at 179.40 and 176.29 ppm with an approximately intensity ratio of 2:1 in downfield, which can be assigned to the carbonyl groups of $\mu_{1,3}$-OAc (**IIIa**) and $\mu_{1,1}$-OAc (**IIIb**), respectively. Although the two binding modes of acetate in $[Zn_2(bdmap)(\mu_{1,1}\text{-OAc})(\mu_{1,3}\text{-OAc})_2]_2$ failed to resolve,[12] in our case, they were separated clearly in about 3.1 ppm. The NMR spectrum of **1** was also recorded and shown in Figure 3c, the resonance peaks at

Scheme 1. Resonance Structures of Chelating Mode

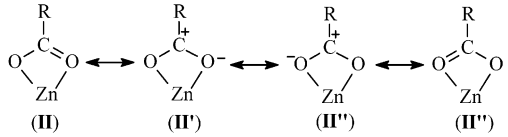

180.66 and 178.91 ppm were assigned to the two carbonyls of acetate. It is worthy of note that the chemical shifts of monodentate and bidentate modes undergo about 8 and 4 ppm upfield shift, respectively, as comparison with the chelating mode. These provide a potential method to diagnose the binding modes of carboxylate groups, especially the chelating and bridging modes. Why the carbonyl chemical shift is at 184.35 ppm for chelating bidentate complex $Zn(OAc)_2(H_2O)$ remains unclear. Nevertheless, this may be related to the electronic effect of the binding metal. The resonance structures of chelating mode can be expressed in Scheme 1. The structures of **II′** and **II″** may be dominant. The downfield shift of the chelating mode can be interpreted in terms of an increased polarization of the carbonyl bond.[14] Consequently, the carbonyl carbon in **II** becomes more positive and deshielding. A similar case was also found in salicyaldehyde because of forming intramolecular hydrogen bond, in which the carbonyl carbon becomes more positive and results in a downfield shift of ca. 6 ppm in comparison with the parent compound.[26]

Conclusion

Two di- and a tetranuclear zinc−carboxylate complexes have been synthesized and characterized by X-ray. A novel tridentate coordination mode of carboxylate, namely, monodentate and syn−anti bidentate bridges, was found in **3**. The solid-state ^{13}C CP/MAS NMR technique is successfully applied to diagnose the different binding modes of carboxylate in zinc−carboxylate complexes. In five-coordinate environment, the chemical shifts are as follows: chelating mode (184 ppm) > bidentate bridge (180 ppm) > monodentate bridge (176 ppm). The correlations between the ^{13}C NMR chemical shifts and carboxylate binding modes provide a useful method in diagnosis of the coordination modes of carboxylate in zinc−carboxylate complexes and zinc−protein.

Acknowledgment. This work was financially supported by a grant from the State Education Department for Returned Scientists from Abroad and NSF of Guangdong Province (B.-H.Y.), and HK- RGC (X.-Y.L.).

Supporting Information Available: X-ray crystallographic file in CIF format for the structure determination of **1**−**3**. This material is available free of charge via the Internet at http://pubs.acs.org.

IC025806+

(25) Ishioka, T.; Murata, A.; Kitagawa, Y.; Nakamura, K. T. *Acta Crystallogr*. **1997**, *C53*, 1029.

(26) Breimaier, E.; Voelter, W. *Carbon-13 NMR Spectroscopy*; VCH Publishers: New York, 1990; p 110.